Some Phenothiazinyl-thiazolyl-hydrazine Derivatives as Corrosion Inhibitors for Carbon Steel in 1.0 M HCl: Electrochemical, SEM-EDX and DFT Investigations

Simona Varvara[1,], Luiza Găină[2], Roxana Bostan[1], Florin Popa[3], Adriana Grozav[4]*

[1] Department of Exact Sciences and Engineering, "1 Decembrie 1918" University, 15-17 Unirii St., 510009 Alba-Iulia, Romania
[2] Department of Organic Chemistry, "Babes-Bolyai" University, 11 Arany Janos St., 400028 Cluj-Napoca, Romania
[3] Materials Science and Engineering Department, Technical University of Cluj-Napoca, 103-105 Muncii Avenue, 400641, Cluj-Napoca, Romania
[4] Department of Organic Chemistry, Faculty of Pharmacy, "Iuliu Haţieganu" University of Medicine and Pharmacy, 8 Victor Babes, 400012 Cluj-Napoca, Romania
*E-mail: svarvara@uab.ro

The inhibition proprieties of two phenothiazinyl-thiazolyl-hydrazine derivatives, namely *(E)-ethyl 2-(2-((10-ethyl-10H-phenothiazin-3-yl)methylene)hydrazinyl)thiazole-4-carboxylate* (CxTP) and *(E)-10-ethyl-3-((2-(4-phenyl thiazol-2-yl)hydrazono)methyl)-10H-phenothiazine* (PhTP) on carbon steel corrosion in 1.0 M HCl solution were studied at various concentrations, temperatures and exposure times using electrochemical techniques, SEM-EDX and quantum chemical calculations. Potentiodynamic polarization revealed that the phenothiazinyl-thiazolyl-hydrazine derivatives act as mixed-type corrosion inhibitors; their inhibition efficiency increases with increasing the inhibitors concentration (91.6% at the optimal concentration of 150 μM for CxTP) and slightly decreases at elevated temperatures and after 24 hours exposure to the corrosive solution. Based on the electrochemical impedance spectroscopy results, two suitable structural models of the carbon steel/1.0 M HCl interface were proposed to describe the processes taking place in the absence and in the presence of the organic inhibitors, respectively. The adsorption of the organic inhibitors on carbon steel surface obey Langmuir isotherm. SEM-EDX investigations confirmed that the phenothiazinyl-thiazolyl-hydrazine derivatives are able to significantly retard the carbon steel dissolution. Density functional theory was used to understand the nature of the interactions between the protonated organic molecules and the metallic surface.

1. INTRODUCTION

Carbon steels materials are extensively used in various industries, including automotive, aircraft, petroleum production and refining, marine applications, chemical and defence, since they balance excellent mechanical properties and a reduce cost [1, 2]. Nevertheless, these alloys are highly susceptible to severe dissolution when exposed to HCl solution during several industrial processes, such as acid pickling, cleaning, descaling and oil well acidizing [3], causing important structural damages and economic losses [4].

The use of corrosion inhibitors is one of the most convenient and cost-effective strategy to minimize the steel dissolution in acid media. As result, numerous organic compounds containing heteroatoms with electron lone pair (P, N, S, O), conjugated multiple π-bonds and/or aromatic rings in their molecular structures have been reported as effective inhibitors for steel corrosion in HCl media. The inhibiting properties of these organic inhibitors is usually attributed to their adsorption on the metal surface *via* different mechanisms, involving coordinate covalent bond (chemical adsorption) and/or electrostatic interaction between the organic molecule and the metal (physical adsorption) [5, 6]. However, the adsorption process is rather complex and depends on several factors, including the nature and charge of the metal, the electrolyte type and the electronic properties of the organic compound, such as steric effects, electronic density of the donor atoms and the orbital character of the donating electrons, aromaticity, the presence of different functional groups, *i.e.* -CHO, -N=N-, R-OH etc. [7, 8]. In many cases, the inhibiting efficiency of the heterocyclic compounds was found to increase with the number of the electron-rich structures, due to their improved ability to share the lone pair electrons with the metal substrate [7]. Consequently, many organic molecules possessing donor atoms and various functional groups in their core, *i.e.* mercapto-functionalized thiadiazole derivatives [9-11], Schiff bases [12-16], pyranpyrazole derivatives [17], thiocarbohydrazides [18], thiazolo-pyrimidine derivatives [19], phenothiazine derivatives [20-22], phenylthiazole derivatives [23] and hydrazide derivatives [24] have shown high inhibition effectiveness for steel corrosion in acid media.

Phenothiazinyl-thiazolyl-hydrazine derivatives represent a class of heterocyclic compounds obtained by assembling the hydrazino-thiazolyl group and the phenothiazine nucleus in the same molecular structure [25], which have recently shown to present antiproliferative activity against tumour cell. Phenothiazinyl-thiazolyl-hydrazine derivatives possess several anchoring sites suitable for surface bonding, *i.e.* N and S atoms with lone *n* and *p* electrons from the phenothiazine core and hydrazino-thiazolyl group, which make this class of organic compounds proper candidates for corrosion inhibition. To the best of our knowledge, the anticorrosive properties of any phenothiazinyl-thiazolyl-hydrazine derivative against steel have not been experimentally investigated and reported, yet.

The aim of the present work is to study the inhibitive properties of two phenothiazinyl-thiazolyl-hydrazine derivatives on carbon steel corrosion in 1.0 M HCl solution, using potentiodynamic polarization, electrochemical impedance spectroscopy and SEM-EDX investigations. In addition, quantum chemical calculation method was applied to explain the interactions between the organic molecules and the carbon steel surface and to assess the corrosion inhibition mechanism. It

should be also mentioned that one of the investigated phenothiazinyl-thiazolyl-hydrazine derivative is a newly synthetized compound that has been reported and characterized for the first time in this paper.

2. EXPERIMENTAL

2.1. Reagents

The corrosive blank solution of 1.0 M HCl was prepared by dilution of the analytical grade 37% reagent (Merck) with double distilled water.

The phenothiazinyl-thiazolyl-hydrazine derivatives proposed as corrosion inhibitors in the present study were synthetized according to a procedure previously reported [25]. The molecular structures of the organic compounds are shown in Fig. 1.
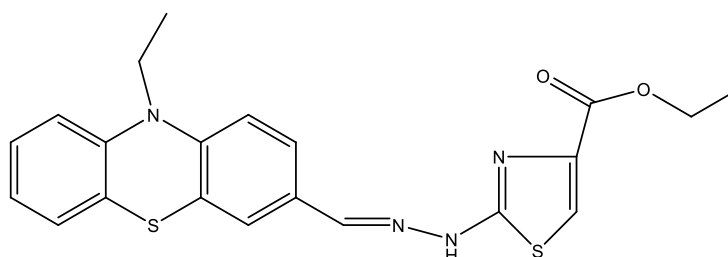
(E)-ethyl2-(2-((10-ethyl-10H-phenothiazin-3-yl)methylene)hydrazinyl)thiazole-4-carboxylate (**CxTP**)
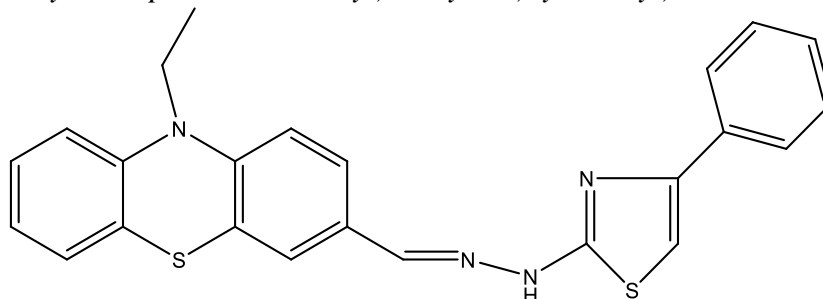
(E)-10-ethyl-3-((2-(4-phenyl thiazol-2-yl)hydrazono)methyl)-10H-phenothiazine **(PhTP)**

Figure 1. Chemical structures of the investigated phenothiazinyl-thiazolyl-hydrazine derivatives

The chemical and structural characterisation of PhTP was formerly described [25]. Instead, CxTP is a newly synthetized compound which has never been reported. Therefore, after its synthesis, it was fully characterized by spectroscopic measurements. The melting point was determined with an Electrothermal IA 9200 digital melting point apparatus and is uncorrected. Elemental analysis was performed using a Vario EL III instrument and ^{1}H NMR spectra was recorded in DMSO-d6 on a WM-400 MHz Bruker NMR spectrometer. The results of the spectroscopic investigations performed on CxTP are presented below.

(E)-ethyl2-(2-((10-ethyl-10H-phenothiazin-3-yl)methylene)hydrazinyl)thiazole-4-carboxylate
Purification by recrystallization from ethanol. Yellow crystals, yield 72% (0.3 g), m.p.[204-205]˚C

^{1}H NMR (400 MHz, DMSO d$_6$) δ (ppm): 1.31 (t, 3H, ^{3}J = 7.3 Hz, -CH$_3$), 1.44 (t, 3H, ^{3}J = 7.1 Hz, -CH$_3$), 3.94 (q, 2H, ^{3}J = 7.1 Hz, N-CH$_2$), 4.31 (q, 2H, ^{3}J = 7.3 Hz, O-CH$_2$), 6.18 (s, 1H, Th-H$_5$),

6.82 (d, 1H, ^3J = 8.6 Hz, H_1), 6.9 (d,1H, ^3J = 7.6 Hz, H_9), 6.91 (t, 1H, ^3J = 7.6 Hz, H_7), 7.14 (dd, 1H, ^3J = 7.6 Hz, H_6), 7.18 (t, 1H, ^3J = 7.6 Hz, H_8), 7.39 (dd, 1H, ^3J = 8.6 Hz, H_2), 7.45 (s, 1H, H_4), 7.81 (s, 1H, CH=N), 9.53 (s, 1H, -NH).

Anal. Calcd. for $C_{21}H_{20}N_4O_2S_2$ (%): C, 59.41; H, 4.75; N, 13.20; S, 15.11. Found (%): C, 59.85; H, 4.71; N, 13.24; S, 15.17.

Due to low solubility of the phenothiazinyl-thiazolyl-hydrazine derivatives in water, in order to prepare solutions containing different concentrations of inhibitors, appropriate weighted amounts of organic compounds were firstly dissolved in 10 mL mixture of ethanol and acetone (3:1, *v:v*). Then, the blank solution was added to obtain 100 mL inhibitor-containing solutions, in which the phenothiazinyl-thiazolyl-hydrazine concentrations lay in the range from 25 to 150 μM.

2.2. Electrochemical measurements

All electrochemical experiments were conducted in a three-electrode glass cell. A carbon steel cylinder (S=0.5 cm^2) embedded in epoxy resin (Buhler, Epoxycure^{TM}) was used as working electrode. The counter-electrode was made of a large platinum foil, whilst a calomel electrode in saturated KCl (SCE) was used as reference electrode. The chemical composition of carbon steel was as follows (wt. %): 0.37 C, 0.47 Mn, 0.01 P, 0.04 Si, 0.029 S and balance Fe.

Prior to each experiment, the surface of C-steel was prepared via an abrading procedure, using successive grade of silicon carbide paper grit (from 600 up to 2400), rinsed with distilled water and ethanol and then immediately inserted into a glass-cell containing 100 mL of electrolyte solution.

All electrochemical measurements were performed at open-circuit potential after 1-hour immersion of C-steel electrode in 1.0 M HCl solution, in the absence and presence of the inhibitors. A PARSTAT model 2273 potentiostat was used for electrochemical measurements. The corrosion tests were performed in the electrolytes, under non-stirred and naturally aerated conditions at room temperature (20^0 C).

Electrochemical impedance spectroscopy (EIS) measurements were carried out in the frequency range from 100 kHz to 10 mHz at 10 points per hertz decade with an AC voltage amplitude of ± 10 mV. The impedance data were interpreted based on equivalent electrical circuits using the ZSimpWin V3.21 software for the experimental data fitting.

Polarization curves were recorded at constant sweep rate of 10 mV min^{-1}, in a wide potential range of ± 250 mV *vs.* OCP from the cathodic to the anodic direction. In order to determine the influence of the temperature on the C-steel corrosion rate, polarisation measurements were also performed at various temperatures, ranging from 25^0 C to 55^0 C.

2.3. SEM–EDX measurements

For morphological studies, the C-steel surface was prepared by immersing the electrodes during 6 h in 1.0 M HCl, in the absence and in the presence of the organic compounds. Then, the specimens were washed gently with distillated water, carefully dried and characterized without any

further treatment by scanning electron microscopy (SEM). The SEM measurements were performed using a JEOL JSM 5600 LV microscope, equipped with an Oxford Instruments energy dispersive X-ray spectrometer (EDX). The energy of the acceleration beam employed was 15 kV and the given results are 500 × magnifications.

2.4. Quantum chemical calculation

For a better understanding the corrosion inhibition properties on molecular level, the structure of the phenothiazinyl-thiazolyl-hydrazine derivatives and their protonated forms were studied by molecular modelling tools as Density Functional Theory (DFT) using hybrid B3LYP, 6-31G* [26] offered by Spartan 06 software.

3. RESULTS AND DISCUSSION

3.1. Electrochemical impedance spectroscopy
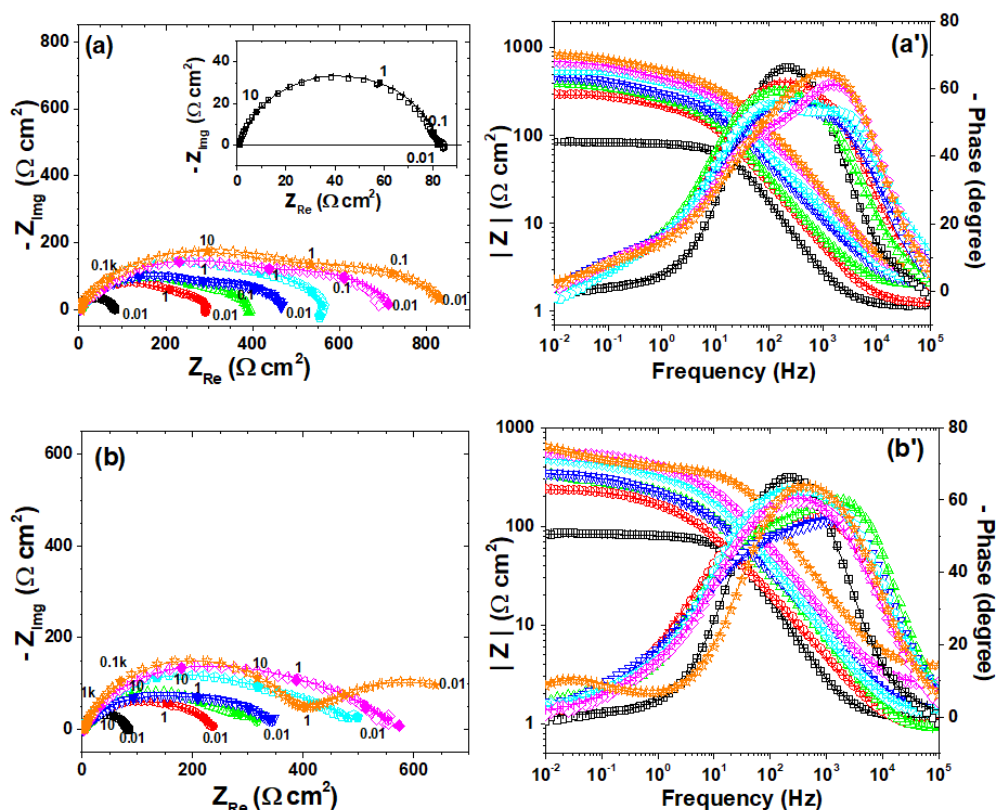
3.1.1. Influence of the inhibitors concentration

Figure 2. Nyquist diagrams (a, b) and Bode plots (a', b') recorded on C-steel surface in 1.0 M HCl solution in the absence (□) and in the presence of different concentrations of phenothiazinyl-thiazolyl-hydrazine derivatives (μM): 25 (○); 50 (△); 75 (▽); 100 (△); 125 (◇); 150 (   ). The insert presents the Nyquist diagram for C-steel corrosion in 1.0 M HCl in enlarged scale (a). Symbol (—+—) corresponds to the fitted data. The numbers in Nyquist diagrams (a, b) refer to frequency in Hz.

Fig. 2 shows the Nyquist diagrams for C-steel after 1 h immersion in 1.0 M HCl solution in the absence and presence of different concentrations of organic inhibitors at room temperature (20 ^{0}C).

In the blank solution, the impedance spectra consist of a capacitive loop at high to medium frequencies, followed by a small inductive loop in the low-frequency region. The addition of the organic compounds in the corrosive solution changes the impedance response of C-steel surface. Thus, two depressed capacitive loops although not always very well-separated could be observed in the impedance spectra of C-steel exposed to inhibitor-containing solutions. The first capacitive loop appearing at high frequency region was attributed to the charge transfer process, while the second one at lower frequencies might be related to the adsorption of inhibitor molecules on the metallic surface [27, 28]. As readily seen in Fig. 2, the diameters of the capacitive loops obtained in the presence of CxTP and PhTP are considerably larger than observed in the blank solution and increase markedly with increasing the organic inhibitors concentration. This behaviour points out to an inhibitive effect exerted by the two organic compounds on C-steel corrosion in 1.0 M HCl. It is also worth mentioning that the change in the CxTP and PhTP concentration did not significantly modify the shape of the impedance diagrams suggesting that a similar inhibition mechanism was involved.

Further information on the electrochemical processes occurring at the electrode-solution interface was obtained by the analysis of impedance spectra using suitable electrical equivalent circuits.

Fig. 3a shows the equivalent circuit used for the uninhibited C-steel interface simulation. In this model, R_e denotes the electrolyte resistance, while the parameters R_{ct} and Q_{dl} describe the charge transfer process at the C-steel/1.0 M HCl interface. Although an inductive loop was also observed at low frequencies in the impedance spectra corresponding to uninhibited C-steel, we omitted to further analyse it, since its origin is rather uncertain. A similar approach was used by Bentiss [29], which explained that the low-frequency inductive loop could be attributed to the adsorption of species resulting from the iron dissolution or to the adsorption of the hydrogen.
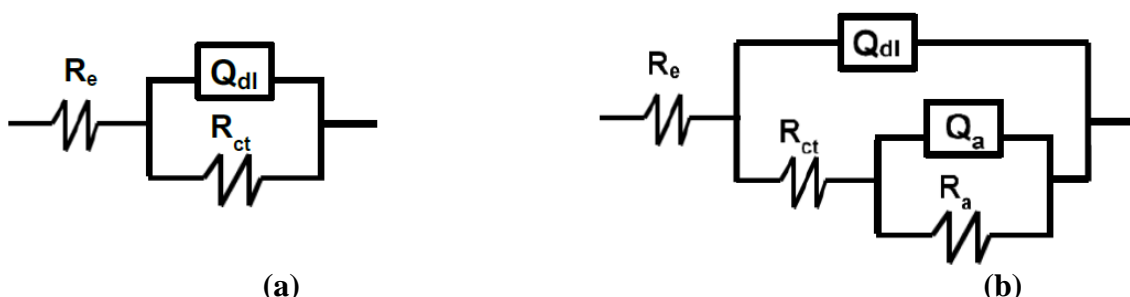

(a)   (b)

Figure 3. Electrical equivalent circuit used to fit the impedance data C-steel corrosion in the absence (a) and in the presence of the phenothiazinyl-thiazolyl-hydrazine derivatives (b)

The proposed equivalent circuit for the interpretation of EIS data obtained in inhibitors-containing solutions is shown in Fig. 3b. In this circuit R_a represents the resistance of the adsorbed inhibitor and Q_a corresponds to the capacitance of the inhibitor film due to the organic compounds adsorption on C-steel surface [15, 27]. Similar equivalent circuits were previously used to simulate the impedance data for C-steel [28] or mild steel [27, 30] corrosion in HCl in the presence of organic inhibitors.

To get more accurate fit of the experimental data, constant phase elements (*CPE*) were substituted for the pure capacitive elements allowing to explain the depressed features of the impedance diagrams, which corresponds to the surface heterogeneities arising from surface roughness, impurities, dislocations, grain boundaries, inhibitor adsorption, porous layers, etc.

The impedance function of *CPE* parameter is given by the following equation [31]:

$$CPE(\omega) = [Q(j\omega)^n]^{-1} \tag{1}$$

where *j* is an imaginary number ($\sqrt{j} = -1$); $\omega = 2\pi f$ is the angular frequency in rad·s^{-1}; *n* is the exponent which defines the character of frequency-dependence (-1 ≤ *n* ≤ 1). The *CPE* could represent a circuit parameter with limiting behaviour as a capacitor for *n* = 1, a resistor for *n* = 0, and an inductor for *n* = -1 [32]. The values of *n* are associated to the non-uniform distribution of current due to the roughness of the metallic surface, the presence of the inhibitor molecules etc.

The proposed equivalent circuits suitably reproduce the impedance data corresponding to C-steel corrosion in the absence and in the presence of the organic compounds as revealed in Fig. 2, where a good agreement between the experimental and simulated data was obtained. The error percentages obtained for each component of the equivalent circuits were generally below 10%, confirming that the experimental data adjusted well to the proposed circuits. The corresponding fitting parameters are given in Table1.

In Table 1 are also listed the values of the pseudo-capacitances associated with the *CPE* parameters, calculated using the following equation:

$$C = \left(R^{1-n}CPE(\omega)\right)^{1/n} \tag{2}$$

As shown in Table 1, the charge-transfer resistance, R_{ct} values increase gradually with increasing the phenothiazinyl-thiazolyl-hydrazine derivatives concentration and reach their maximum values of 469.7 Ω cm^2 and 390.6 Ω cm^2 at the concentration of 150 μM, in the presence of CxTP and PhTP, respectively. The higher values of R_{ct} obtained in the presence of the organic compounds as compared to the blank solution (R_{ct} = 81.1 Ω cm^2) should be related to a slower corroding system [24] due to the inhibitors adsorption on the C-steel surface.

In the absence of the inhibitors, the double layer capacitance, C_{dl} has a relatively high value of 109.7 μF cm^{-2}, which might be explained by the accumulation of corrosion products on the rough C-steel surface. The addition of the organic compounds in the corrosive solution leads to a decrease of the C_{dl} values and this tendency is more pronounced at higher concentrations of inhibitors. The lowest C_{dl} values of 9.5 μF cm^{-2} and 13.8 μF cm^{-2} were obtained at 150 μM, in the presence of CxTP and PhTP, respectively. The decrease of C_{dl} values with increasing the inhibitors concentration may be originated from the decrease of the local dielectric constant and/or the increase in thickness of the electrical double layer confirming that the organic compounds act *via* adsorption on C-steel surface [30, 33].

The R_a values progressively increase with the concentration of the phenothiazinyl-thiazolyl-hydrazine derivatives, while simultaneously the adsorption capacitance, C_a has generally a decreasing trend. It might be assumed that the adsorption of the organic inhibitors on C-steel surface hinders the formation of the corrosion products providing enhanced protection to metallic surface. This explains

why the corrosion products were significantly diminished on C-steel surface, as proved by SEM micrographs (Fig. 10).

Table 1. Electrochemical parameters of C-steel corrosion in 1.0 M HCl solution obtained in the absence and in the presence of various concentrations of phenothiazinyl-thiazolyl-hydrazine derivatives at 20^0 C

Inhibitor	C_{Inh}	R_e	R_{ct}	Q_{dl}	n_1	C_{dl}	R_a	Q_a	n_2	C_a	R_p	z
	(μM)	(Ω cm^2)	(Ω cm^2)	(μF s^{n-1}cm^{-2})		(μF cm^{-2})	(Ω cm^2)	(mF s^{n-1}cm^{-2})		(mF cm^{-2})	(Ω cm^2)	(%)
Blank	0	1.1	81.1	193.3	0.88	109.7	-	-	-	-	81.1	-
CxTP	25	1.2	216.4	228.3	0.77	92.9	85.5	6.9	0.66	5.3	301.9	73.1
	50	1.9	266.4	213.6	0.72	70.1	129.0	5.2	0.68	4.3	395.4	79.5
	75	1.9	309.1	194.7	0.73	68.9	168.1	4.5	0.69	4.0	477.2	83.0
	100	2.2	342.5	140.7	0.73	45.8	236.5	2.1	0.69	1.5	579.0	86.0
	125	2.2	408.9	85.7	0.73	24.8	298.4	2.0	0.68	1.6	707.3	88.5
	150	2.7	469.7	34.9	0.76	9.5	398.0	1.5	0.62	1.1	867.5	90.7
PhTP	25	0.8	168.2	494.9	0.70	170.5	70.7	4.8	0.62	2.5	238.9	66.1
	50	0.7	194.7	255.6	0.75	94.0	105.2	2.7	0.56	1.0	299.9	73.0
	75	1.2	208.0	304.2	0.69	88.0	147.9	3.1	0.59	1.8	355.9	77.2
	100	1.3	292.5	140.5	0.78	57.1	215.4	3.2	0.51	2.3	507.9	84.0
	125	2.3	335.2	109.9	0.77	41.0	183.8	2.2	0.53	0.9	569.0	85.7
	150	3.7	390.6	33.5	0.83	13.8	392.4	9.96	0.61	23.8	783.0	89.6

In the blank solution, the polarization resistance, R_p consists of the charge transfer resistance, while in the presence of the organic inhibitors, the sum of R_{ct} and R_a is equivalent to R_p [28].

The related inhibition efficiency, z was calculated using the R_p values according to the following equation:

$$z(\%) = \frac{R_p - R_p^0}{R_p} \times 100 \qquad (3)$$

where R_p and R_p^0 are the polarization resistances in the corrosive solution with and without inhibitors, respectively.

As reported in Table 1, the increase of organic compounds concentration significantly enhances the R_p values, and consequently improves the inhibition efficiency, until reaching the maximum values of 90.7% for CxTP and 89.6% for PhTP, at their optimum concentration (150 μM).

3.1.2. Influence of the immersion time

To assess the short time-evolution of the inhibitor-metal system, EIS measurements were carried out at the open-circuit potential during 24 h of C-steel exposure to 1.0 M HCl in the absence

and in the presence of the organic inhibitors, at the optimum concentration of 150 µM. The impedance data were collected every 2 h at room temperature and several experimental results are presented in Fig. 4. The fitted curves represented by lines with crosses are shown together with the experimental data represented by symbols.
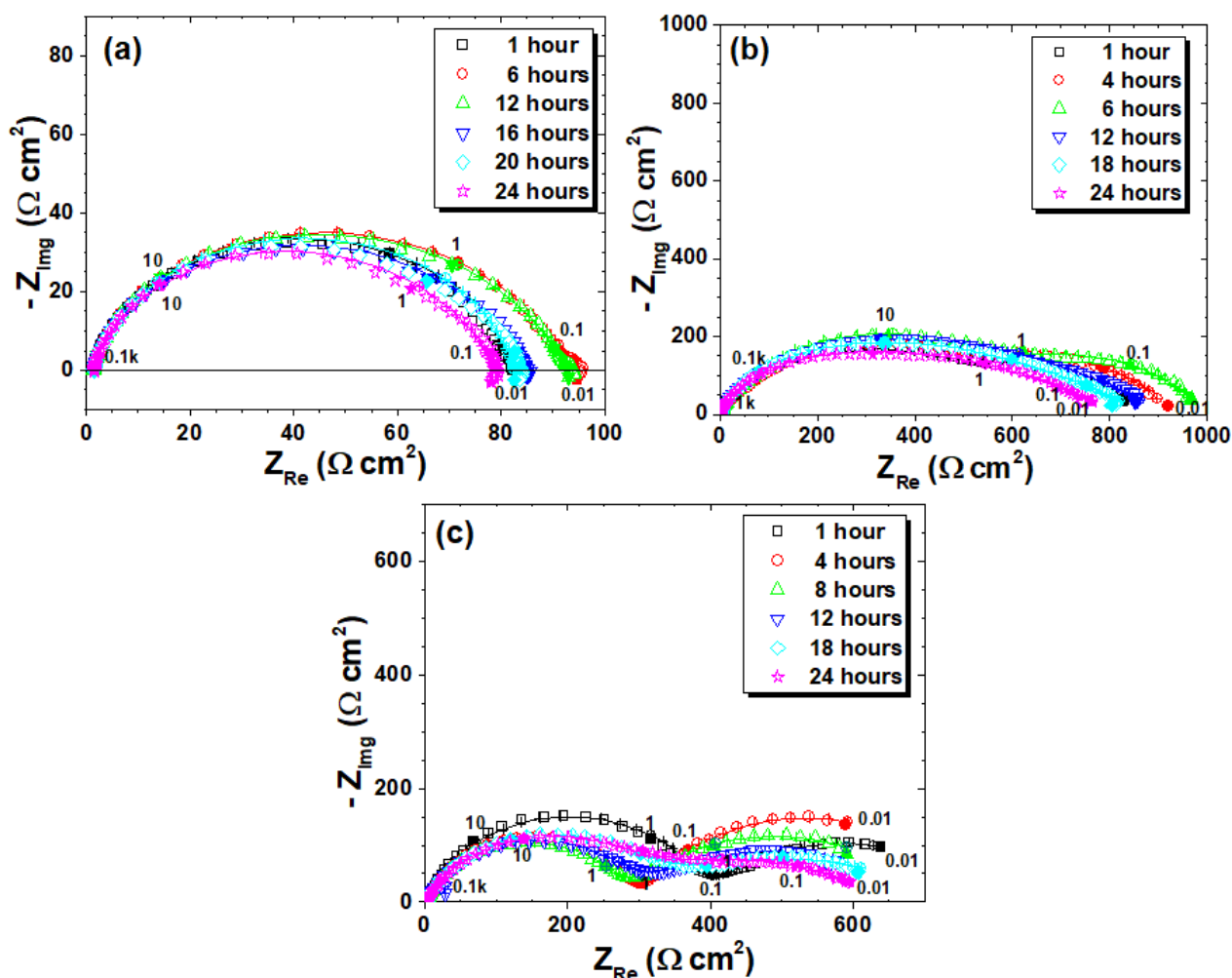

Figure 4. Typical Nyquist diagrams for C-steel corrosion at different immersion times in 1.0 M HCl solution in the absence (a) and in the presence of 150 µM organic inhibitors: CxTP (b) and PhTP (c). Symbol (—+—) corresponds to the fitted data. The numbers in Nyquist diagrams refer to frequency in Hz

As observed in Fig. 4 the shapes of the impedance diagrams obtained at different immersion time in electrolytes containing phenothiazinyl-thiazolyl-hydrazine derivatives are similar with those recorded after 1 hour-exposure, but the diameters of the capacitive loops increase.

The change of the R_p values with the immersion time observed in the presence of the organic inhibitors confirm that their protective effectiveness on C-steel corrosion is time-dependent (Fig. 5a).
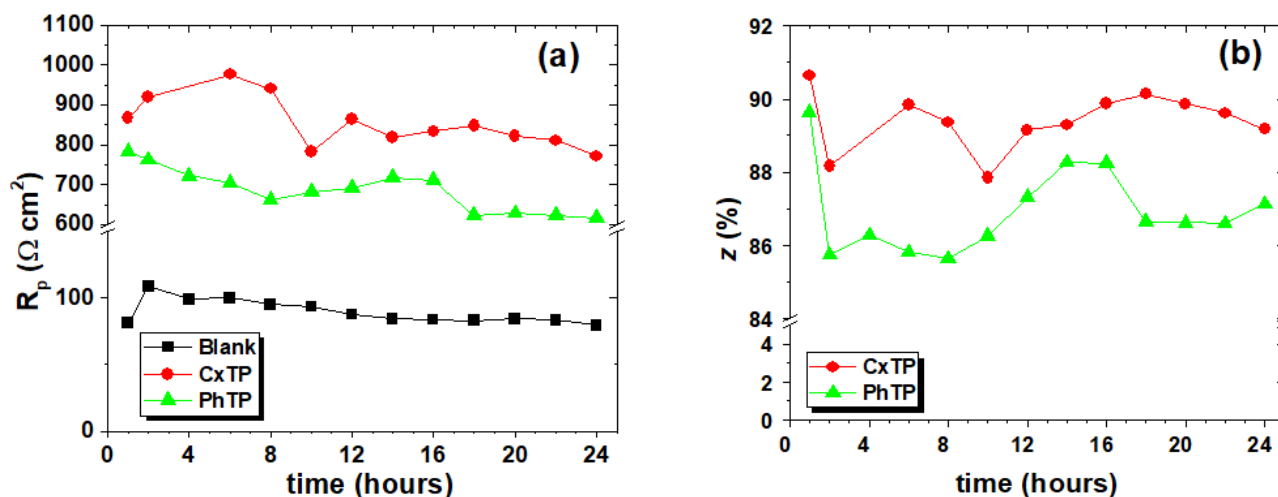
Figure 5. Variation of the polarisation resistance (a) and inhibition efficiency (b) during the immersion time in 1.0 M HCl solution

Disregarding the exposure to the corrosive solution, CxTP exerts a better protective effect on C-steel surface as compared to PhTP. The highest R_p value was obtained in the presence of 150 µM CxTP after 6 h immersion in the corrosive solution, while at longer exposure, the polarization resistance starts decreasing, as illustrated in Fig. 5a. A rather reducing trend of the R_p values over time was also noticed in the presence of 150 µM PhTP.

Although the anticorrosive properties of the investigated phenothiazinyl-thiazolyl-hydrazine derivatives decrease slightly over time, as observed in Fig. 5b, the z values remain rather high even after 24 h of exposure to 1.0 M HCl, *i.e.* 89.2% for CxTP and 87.1% for PhTP.

3.2. Polarization measurements

3.2.1. Influence of the inhibitor concentration

Fig. 6 shows the cathodic and anodic polarization plots of C-steel immersed in 1.0 M HCl solution, in the absence and presence of different concentrations of organic inhibitors.

It is shown in Fig. 6 that the investigated organic compounds reduce the anodic and cathodic current densities compared to the blank solution, while the corrosion potentials were shifted toward more negative values. Likewise, the addition of increasing concentrations of inhibitors suppressed to greater extents the cathodic hydrogen evolution than the anodic iron dissolution.

In order to get information about the kinetics of the metal dissolution process, the related electrochemical parameters, *i.e.* corrosion potential (E_{corr}), cathodic (β_c) and anodic (β_a) Tafel slopes, corrosion current density (i_{corr}) were calculated by extrapolation of the linear part of the current-potential curves to the corrosion potential. The obtained parameters are presented in Table 2.

In Table 2 are also listed the values of the inhibition efficiency (z) calculated according to the following equation:

$$z(\%) = \frac{i^{0}_{\mathrm{corr}} - i_{\mathrm{corr}}}{i^{0}_{\mathrm{corr}}} \cdot 100 \qquad\qquad\qquad (4)$$

where i^{0}_{corr} and i_{corr} are the corrosion current density values without and with inhibitor, respectively.
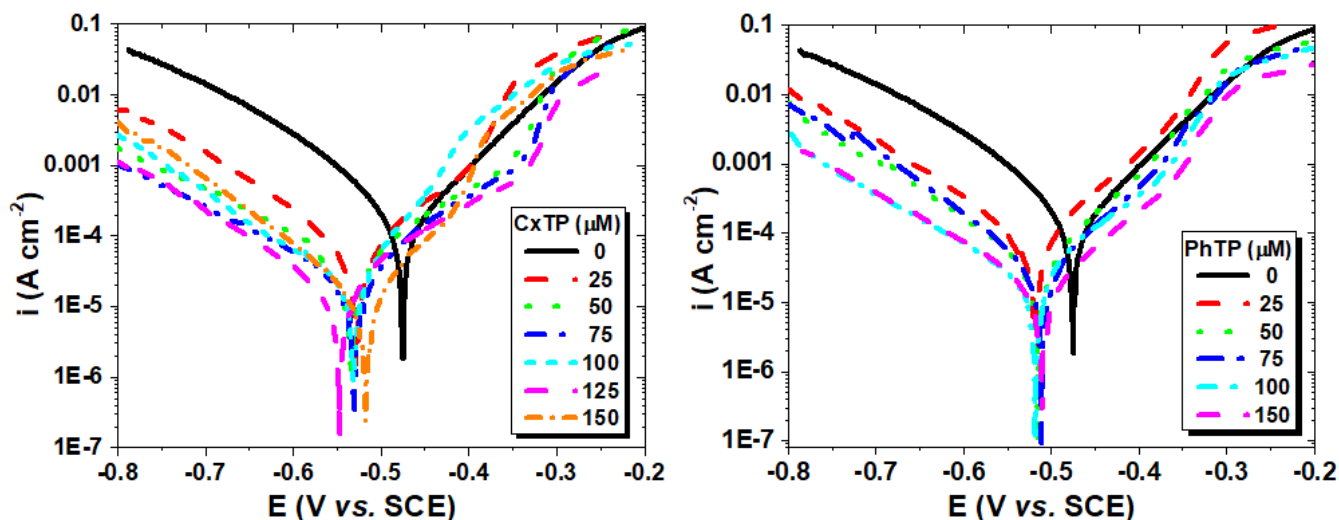

Figure 6. Polarization curves for C-steel immersed in 1.0 M HCl solution containing different concentrations of phenothiazinyl-thiazolyl-hydrazine derivatives at 20^0C

Table 2. Electrochemical corrosion parameters obtained from the polarization curves in the absence and in the presence of various concentrations of phenothiazinyl-thiazolyl-hydrazine derivatives at 20^0 C

Inhibitor	c_{Inh} (µM)	E_{corr} (mV *vs.* SCE)	i_{corr} (µA cm^{-2})	$|\beta_c|$ (mV dec^{-1})	β_a (mV dec^{-1})	z (%)
Blank	0	-475.1	160.8	103.7	92.3	-
CxTP	25	-527.8	66.6	126.4	113.2	58.6
	50	-534.2	36.1	124.8	107.6	77.5
	75	-530.2	25.0	170.1	95.8	84.5
	100	-531.7	23.7	126.5	60.3	85.3
	125	-547.1	21.8	150.2	125.5	86.4
	150	-517.4	13.5	110.8	81.5	91.6
PhTP	25	-505.5	74.0	123.2	89.5	54.0
	50	-508.2	37.3	127.1	87.7	76.8
	75	-511.1	30.8	109.9	93.2	80.9
	100	-518.3	27.0	172.5	102.4	83.2
	150	-510.8	19.8	146.9	107.0	87.7

From Table 2, it is obvious that the addition of the phenothiazinyl-thiazolyl-hydrazine derivatives causes an important decrease of the corrosion current density values and the extent of

reduction is concentration-dependent. Disregarding the nature of the organic inhibitors, as their concentration increases, the corrosion current density decreases progressively and the lowest values were obtained at the concentration of 150 μM. Correspondingly, the inhibition efficiency values increase with increasing the inhibitors concentration and were in the range of 58.6 - 91.6% for CxTP and 54.0 - 87.7% for PhTP, respectively. These results confirm that the two phenothiazinyl-thiazolyl-hydrazine compounds act as efficient inhibitors on C-steel corrosion in 1.0 M HCl solution, particularly at high concentrations. The greatest anticorrosive effectiveness was obtained in the presence of CxTP, in accordance with the experimental data obtained from EIS.

Furthermore, a shift of E_{corr} towards more negative values takes place in the presence of the organic inhibitors. Compared to the blank solution, the corrosion potential of C-steel shifts about 42-72 mV cathodically in the presence of CxTP, while PhTP causes a negative displacement of E_{corr} values in the range of 30-43 mV. According to the literature [34], an inhibitor could be classified as cathodic or anodic if the displacement of the corrosion potential is more than 85 mV with respect to the corrosion potential of the blank solution. The obtained results suggest that the two phenothiazinyl-thiazolyl-hydrazine derivatives might be classified as mixed-type inhibitors of C-steel corrosion with a predominant cathodic effectiveness.

Regarding the Tafel slope, it can be noticed that both anodic (β_a) and cathodic (β_c) kinetics are modified in the presence of the inhibitors. These results confirm the ability of the organic compounds to reduce the anodic iron dissolution and to retard the hydrogen evolution reaction, acting as mixed-type inhibitors. This is likely due to the adsorption of the inhibitors on C-steel forming a barrier film that blocks the reaction sites of the metal surface [23, 35]. As expected, a higher coverage of organic compounds on C-steel surface was obtained in solutions containing higher concentrations of inhibitors.

The parallel cathodic Tafel curves in Fig. 6 suggest that the hydrogen evolution is activation-controlled and the adsorption of the phenothiazinyl-thiazolyl-hydrazine derivatives merely decreases the actual surface area available for the reduction of H^+ ions, without affecting the cathodic reaction mechanism.

In the anodic domain, for potentials higher than about -400 to -350 mV *vs.* SCE, a steep increase of the anodic current density could be observed on the polarisation curves obtained in the presence of the organic compounds. This behaviour is more evident at higher concentrations of inhibitors and particularly in the presence of CxTP. A similar phenomenon was noticed for the steel corrosion in HCl [6, 7] or H_3PO_4 solutions [36] in the presence of organic inhibitors. It was attributed either to the desorption of the absorbed inhibitor [37] or to the equilibrium between the adsorption and desorption of the inhibitor on the metallic surface [6].

3.2.2. Influence of temperature

The influence of temperature on the inhibited acid-metal reaction is rather complex since various changes might occur on the metallic surface, *i.e.* rapid etching and desorption of inhibitor or even the decomposition or rearrangement of its molecules [29, 38].

To investigate the effect of the temperature and to determine the activation energies of the corrosion process, potentiodynamic polarization experiments were performed on C-steel surface in 1.0 M HCl solution, in the temperature range of 25 to 55^{0}C in absence and presence of the optimum concentration of phenothiazinyl-thiazolyl-hydrazine derivatives (150 µM). The obtained polarisation curves are depicted in Fig. 7.
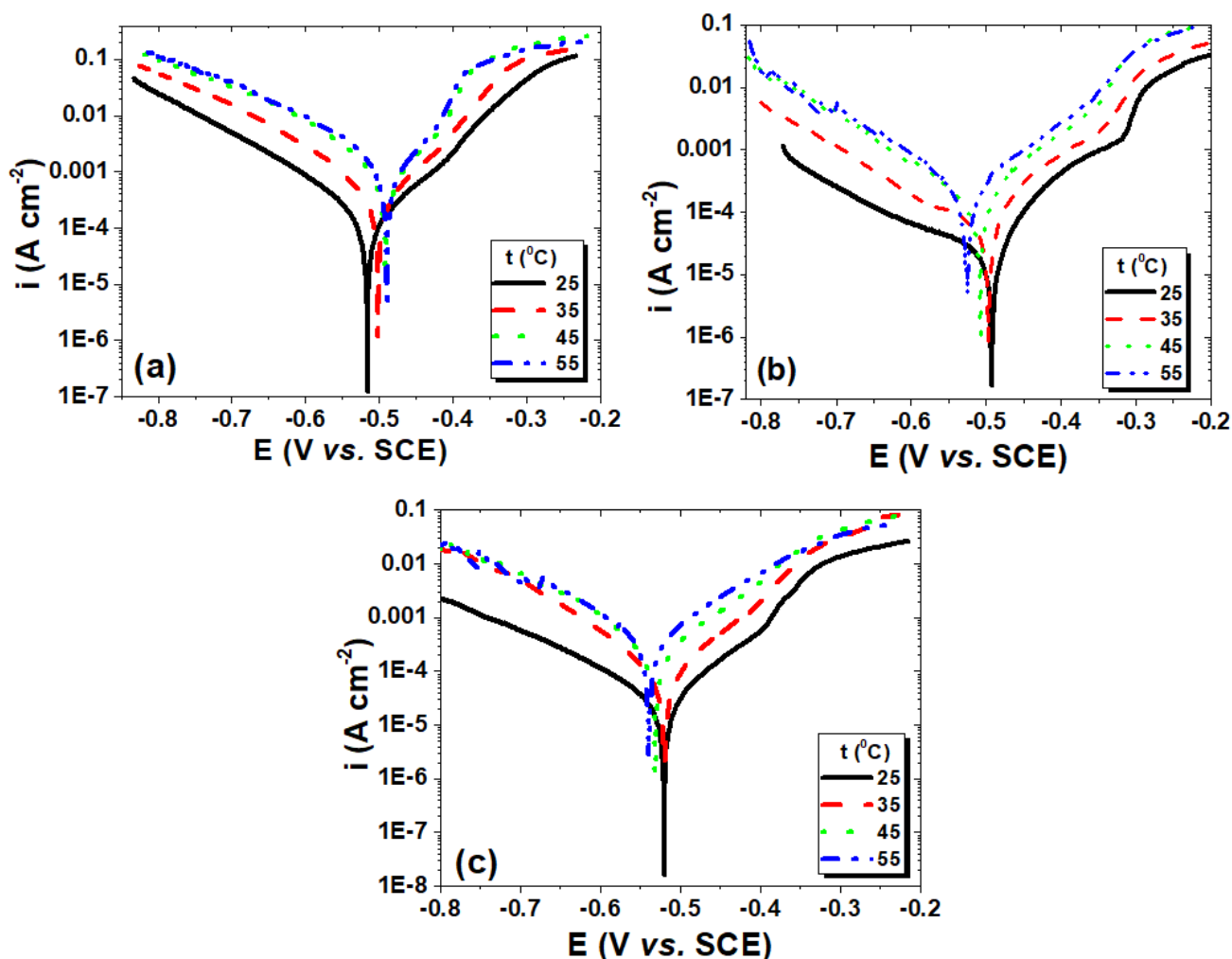

Figure 7. Polarisation curves for C-steel in 1.0 M HCl solution at different temperatures in the absence (a) and in the presence of 150 µM organic inhibitors: CxTP (b) and PhTP (c)

As shown in Fig. 7, the anodic and cathodic current densities increase under the accelerating effect of the temperature in the blank and inhibited solutions. The rates of the metal dissolution and hydrogen evolution are both enhanced by the temperature raising, but to a much lower extent in inhibitors-containing solutions.

Table 3 summarizes the corrosion kinetic parameters determined by Tafel extrapolation of the polarization curves at various temperatures.

Table 3. Effect of temperature on the electrochemical parameters of C-steel corrosion in 1.0 M HCl solution in the absence and in the presence of 150 µM phenothiazinyl-thiazolyl-hydrazine derivatives

Inhibitor	t (^{0}C)	E_{corr} (mV vs. SCE)	i_{corr} (µA cm^{-2})	$|\beta_c|$ (mV dec^{-1})	β_a (mV dec^{-1})	z (%)
Blank	25	-516.2	171	119.3	100.9	-
	35	-501.9	390	111.9	97.6	-
	45	-491.5	1108.2	121.5	109.1	-
	55	-489.4	1309.2	120.4	102.6	-
CxTP	25	-503.3	22.1	178.9	99.6	87.1
	35	-505.5	64.5	212.9	91.4	83.5
	45	-508.6	200.3	188.1	112.4	81.9
	55	-525.7	309.4	151.1	133.8	76.4
PhTP	25	-520.3	34.0	144.3	98.5	79.9
	35	-519.8	94.0	104.8	89.2	75.9
	45	-531.4	252.2	111.9	103.5	77.2
	55	-539.5	477.4	130.9	121.8	63.5

In the blank solution, the i_{corr} values are significantly higher at elevated temperatures, while the E_{corr} shift towards more positive values, indicating that the dissolution rate of the C-steel is greatly enhanced by the temperature raising.

In the presence of the inhibitors, the corrosion current densities also increase with the temperature, but they are much lower compared to the i_{corr} values obtained for the blank solution, at each temperature. Although the corrosion rate is accelerated at elevated temperatures, CxTP and PhTP still present inhibitive properties on C-steel corrosion, in the studied temperature range. These results are consistent with the inhibition efficiency values, which decrease slightly when the temperature increases, but remain quite high of about 81.9% and 77.2% at 45^{0}C in the presence of CxTP and PhTP, respectively. A destabilisation of the adsorbed inhibitor film on the C-steel surface might takes place at elevated temperatures, resulting in a lower coverage [39] and, thus to a higher extent of corrosion.

Further inspection of the data of Table 3 shows that there are no significant changes in the Tafel slopes of the two branches of the polarization curves corresponding to the blank solution, as the temperature increases. Instead, in the presence of the organic inhibitors, both the anodic and cathodic Tafel slopes change with the temperature and this tendency is more pronounced at elevated temperatures.

The activation energy of the corrosion process, E_a could be determined by the Arrhenius equation:

$$i_{corr} = A \, exp\left(-\frac{E_a}{RT}\right) \tag{5}$$

where E_a is the activation energy of the corrosion process, T is the absolute temperature, R is the gas constant, A is the Arrhenius pre-exponential factor and i_{corr} is the corrosion current density.

In Fig. 8 showing the Arrhenius plot of *ln* i_{corr} *vs.* $\frac{1}{T}$, straight lines were obtained in the absence and presence of the two organic compounds, with the slope of $-\frac{E_a}{R}$.
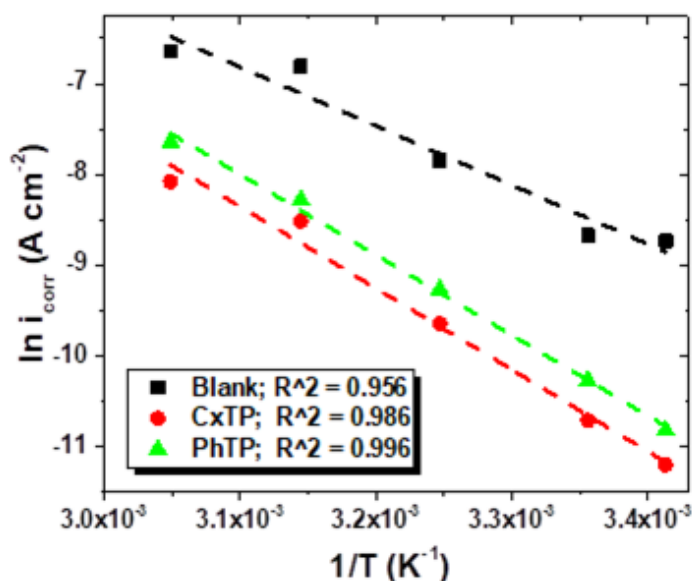

Figure 8. Arrhenius plots for C-steel corrosion in 1.0 M HCl solution in the absence and in the presence of phenothiazinyl-thiazolyl-hydrazine derivatives at the concentration of 150 μM

The calculated activation energy for C-steel corrosion in 1.0 M HCl is 54.2 kJ mol^{-1}, while in the presence of CxTP and PhTP, the obtained E_a values are 74.9 kJ mol^{-1} and 73.8 kJ mol^{-1}, respectively. The higher E_a values obtained in presence of the organic compounds should be associated to a physical barrier for charge and mass transfer created by the adsorbed inhibitor molecules [16, 40]. Considering the specific adsorption of the chloride ions on C-steel surface in the strong acidic electrolyte, it can be assumed that the inhibitors might be electrostatically adsorbed in their protonated forms at the first stage [40], as further explained in Section 3.5. The small difference in the values of the activation energy should be due to the differences in the molecular structure of the protonated phenothiazinyl-thiazolyl-hydrazine derivatives [41]. However, as explained by Zhang [40], the adsorption of an organic molecule could not be considered only as a physical or chemical adsorption phenomenon, since a wide spectrum of conditions, ranging from the dominance of chemisorption or electrostatic effects arises from the other adsorption experimental data.

3.3. Adsorption isotherm

More information on the interaction mechanism between the organic inhibitors and metallic surface could be provided by the adsorption isotherm. For this purpose, a direct relationship between inhibition efficiency (z) and the surface coverage degree ($\theta = z/100$) was assumed for different concentrations of inhibitors.

Among different adsorption isotherms, the Langmuir isotherm is widely used for explaining the adsorptive mechanism of the inhibitors on the metallic surfaces and therefore, it was tested firstly.

According to Langmuir isotherm, the fractional surface coverage, θ is related to the inhibitor concentration, c_{Inh} via the following relation:

$$\frac{c_{Inh}}{\theta} = \frac{1}{K} + c_{Inh} \qquad (6)$$

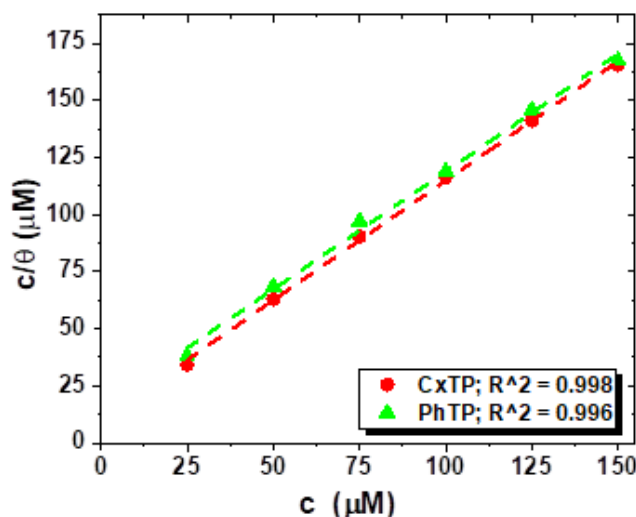where K is the adsorption equilibrium constant.

Figure 9. Langmuir adsorption isotherm of the phenothiazinyl-thiazolyl-hydrazine derivatives on C-steel surface in 1.0 M HCl solution, at 20^0 C

The values of adsorption equilibrium constant, K were calculated from the interception of the straight lines in Fig. 9 and the obtained values are given in Table 4.

The standard free energy of adsorption ΔG^0_{ads} was calculated from the adsorption equilibrium constant, K according to the following equation:

$$K = \frac{1}{55.5} \exp\left(\frac{-\Delta G^0_{ads}}{RT}\right) \qquad (7)$$

where 55.5 represents the molar concentration of water in solution (mol dm^{-3}), R is the gas constant and T is the thermodynamic temperature.

The calculated ΔG^0_{ads} values corresponding to the adsorption of the organic compounds on C-steel in 1.0 M HCl are also depicted in Table 4.

Table 4. Thermodynamic parameters for the adsorption of phenothiazinyl-thiazolyl-hydrazine derivatives on C-steel in 1M HCl solution at 20^0 C

Inhibitor	Slope	K (dm^3 mol^{-1})	$-\Delta G^0_{ads}$ (kJ mol^{-1})
CxTP	1.08	$100.90 \cdot 10^3$	37.84
PhTP	1.02	$63.69 \cdot 10^3$	36.71

It is known that values of ΔG^0_{ads} around - 20 kJ mol^{-1} or less negative are associated with the electrostatic interactions between the charged molecules and charged metal surface (physisorption), while those more negative than - 40 kJ mol^{-1} involve sharing or transfer of electrons from the inhibitor molecules to the metal surface to form coordinate type of bonds (chemisorption).

In the present study, the calculated ΔG^0_{ads} values suggest that the adsorption of the phenothiazinyl-thiazolyl-hydrazine derivatives on C-steel in 1.0 M HCl is a combination of physisorption and chemisorption [13, 42].

The absolute values of ΔG^0_{ads} slightly decrease in the order CxTP > PhTP, in agreement with the range of the inhibition efficiency values obtained from the electrochemical measurements.

A comparison of the inhibitive performance and adsorption mechanism of the studied phenothiazinyl-thiazolyl-hydrazine derivatives with several organic molecules previously described in the literature as efficient inhibitors for C-steel corrosion in 1.0 M HCl solution is given in Table 5.

Table 5. The adsorption mechanism and inhibition efficiency values obtained for several organic inhibitors previously reported as corrosion inhibitors for C-steel in 1.0 M HCl solution

Inhibitor	Optimum Concentration	Highest inhibition efficiency (%)	Adsorption mechanism	Reference
2,5-Bis(4-dimethylaminophenyl)-1,3,4-oxadiazole	1 mM	93%	Chemisorption	[1]
N,N-pentane-2,4-diylidenedipyridin-4-amine		88.0	Chemisorption and Physisorption	[13]
N,N-(3-Benzylidenepentane -2,4-diylidene)dipyridin-4-amine		91.6		
N,N-[3-(4-methoxybenzylidene)pentane-2,4-diylidene] dipyridin-4-amine	400 ppm	90.0		
N,N-[3-(4-chlorobenzylidene)pentane-2,4diylidene] dipyridin-4-amine		83.9		
N,N'-[2,2'-thiocarbonylbis(hydrazine-2,1-diyl)bis(thioxomethylene)] dibenzamide	0.2 mM	96.9 %	Chemisorption	[18]
N,N'-[2,2'-thiocarbonylbis(hydrazine-2,1-diyl)bis(thioxomethylene)]bis(4-methoxy benzamide)		98.2%		
3,5-bis(2-thienylmethyl)-4-amino-1,2,4-triazole	0.1 mM	92.2	Chemisorption	[28]

2-(n-hexylamino)-4-(3'-N,N-dimethylamino-propyl)amino-6-(benzothiazol-2-yl)thio-1,3,5-s-triazine		99.0	Chemisorption and Physisorption	[35]
	1 mM			
2-(n-octylamino)-4-(3'-N,N-simethylaminopropyl) amino-6-(benzothiazol-2-yl)thio-1,3,5-s-triazine		99.3		
2,5-bis(2-thienyl)-1,3,4-thiadiazole		93.70	Chemisorption	[38]
	0.15 mM			
2,5-bis(3-thienyl)-1,3,4-thiadiazole		97.19		
E)-ethyl 2-(2-((10-ethyl-10H-phenothiazin-3-yl)methylene) hydrazinyl)thiazole-4-carboxylate	0.15 mM	91.6	Chemisorption and Physisorption	Present work
(E)-10-ethyl-3-((2-(4-phenyl thiazol-2-yl)hydrazono)methyl)-10H-phenothiazine		87.7		

The data in Table 5 shows that the studied phenothiazinyl-thiazolyl-hydrazine derivatives present similar adsorption mechanism and inhibitive performances with those previously reported for different organic compounds possessing several anchoring sites suitable for surface bonding, *i.e.* certain diquaternary Schiff dibases in the same experimental conditions.

3.4. SEM-EDX investigations

The surface morphology of C-steel specimens after 6 h immersion in 1.0 M HCl solution, in the absence and in the presence of 150 μM phenothiazinyl-thiazolyl-hydrazine derivatives was investigated by SEM.
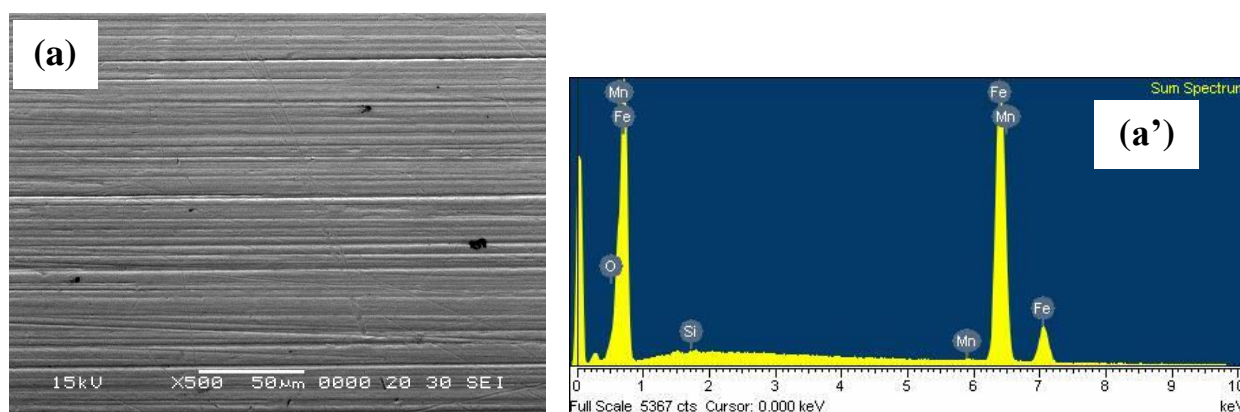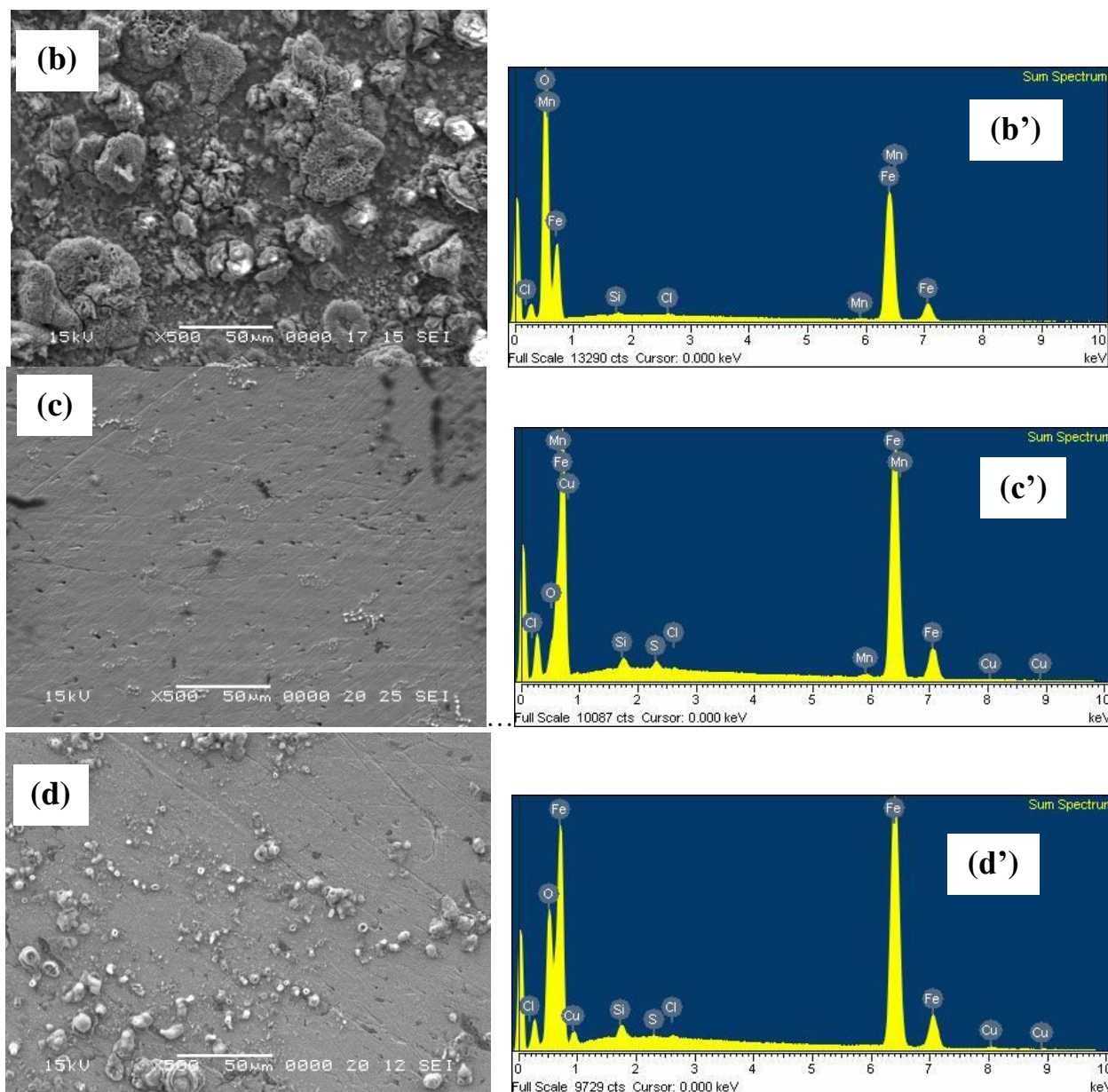
Figure 10. SEM micrographs and EDX spectra of C-steel before (a, a') and after 6 h of immersion in 1.0 M HCl solution in the absence (b, b') and in the presence of 150 μM organic inhibitors: CxTP (c, c') and PhTP (d, d').

Fig. 10a shows the polished surface of C-steel before exposure to the aggressive solution; it reveals some dark spots, already known as non-metallic inclusions and scratches due to the polishing. After 6 h exposure to 1.0 M HCl, C-steel surface appears to be highly corroded due to the aggressive attack of the acid solution (Fig. 10b).

In contrast, in the presence of the organic compounds, the degree of corrosion is markedly reduced and a smoother and less damaged morphology of C-steel surface could be seen in Figs. 10c and 10d. This observation clearly verifies that both, CxTP and PhTP present inhibiting properties on the C-steel corrosion. The organic compounds form a protective adsorbed film on the metallic surface, hindering C-steel dissolution in 1.0 M HCl. However, some corrosion products are still present on the C-steel surface, especially in the presence of PhTP, which has a lower inhibition effectiveness. These

active corrosion zones visible on the C-steel surface in the presence of the organic inhibitors might appear due to the protective film deterioration during the immersion time.

EDX spectra was used to identify the elements present on C-steel surface before and after 6 h exposure to 1.0 M HCl solution, in the absence and in the presence of the organic inhibitors. The obtained results are displayed in Fig. 10. As expected, the formation of iron oxides as corrosion products on the C-steel surface after 6 h immersion in 1.0 M HCl is demonstrated by the appearance of the large O peak on the EDX spectrum. An additional signal for the existence of Cl element on the surface could be also notice in Fig. 10b'.

In the inhibited solutions, the O signal is significantly reduced; the weight percent of O decreases from 36.81% in the blank solution to 6.32% and 16.19% in the presence of CxTP and PhTP, respectively. The highest reduction of the O content noticed in the presence of CxTP (Fig. 10c') endorse its greater inhibiting efficiency over PhTP (Fig. 10d'), in accordance with the results of the electrochemical measurements.

3.5. Quantum chemical calculations

Quantum chemical calculations were carried out to understand the nature of the interactions between the organic molecules and C-steel surface.
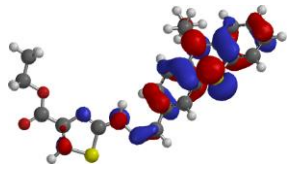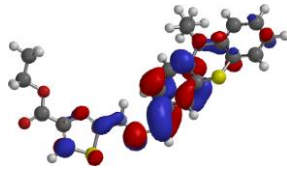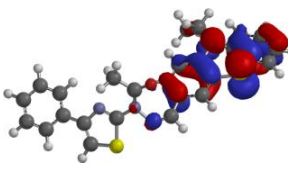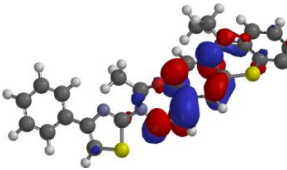
The frontier molecular orbital distributions for the phenothiazinyl-thiazolyl-hydrazine derivatives determined by hybrid DFT functional (B3LYP/6-31G*) basis set are shown in Table 6. The generated lowest energy conformers were further used to calculate the quantum molecular parameters, such as E_{HOMO}, E_{LUMO}, energy gap, ΔE ($E_{LUMO} - E_{HOMO}$), which are also listed in Table 6.

The attempts to correlate the quantum chemical parameters with the experimental inhibition efficiencies indicate that no relationship could be derived from the inhibition performance of the studied organic inhibitors. The expectation was that amongst the two derivatives, the molecule having the highest E_{HOMO} and the lowest E_{LUMO} and ΔE values would provide the best inhibitive properties, but the results attest the contrary [18]. This inconsistency between the quantum chemical parameters and the experimental z data provides a confirmation of the complex nature of interactions that are involved in the corrosion inhibition process [43], including the competing effects, *i.e.* interactions inhibitor molecule-water, inhibitor molecule-metal, metal-water and water-water [18], as well as the protonation reactions.

It is known that the protonation usually occurs in acidic solution containing inhibitors with heteroatoms having lone pair of electrons and the protonated species have been reported to take part in the adsorption process on the metallic surface [44].
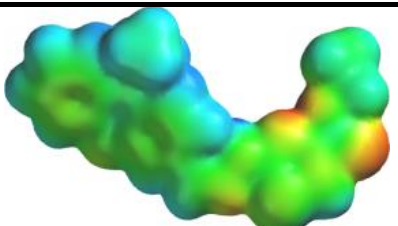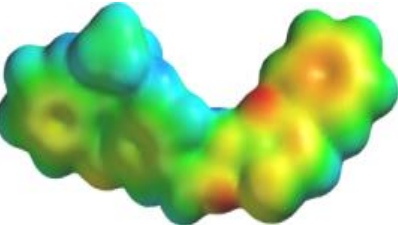
The molecular structure of the investigated phenothiazinyl-thiazolyl-hydrazine derivatives is complex (Fig. 1) and present several sites for protonation, *i.e.* S atom from the phenothiazine group, N and S atoms from the thiazole moiety, N atoms from the hidrazinyl bridge and O atom in the ester moiety.

Table 6. Theoretical quantum chemical parameters of the phenothiazinyl-thiazolyl-hydrazine derivatives and the typical HOMO and LUMO densities distribution

| Molecule	*E* (kcal/mol)	E_{HOMO} (eV)	E_{LUMO} (eV)	ΔE (eV)	HOMO	LUMO
CxTP	-1241270.03	-5.15	-1.48	3.69		
PhTP	-1218594.76	-5.07	-1.39	3.68		

In an attempt to identify the most favourable sites for the protonation of the organic compounds in HCl, the Mulliken, electrostatic and natural atomic charges were calculated and their values are presented in Table 7. The electrostatic potential surfaces corresponding to CxTP and PhTP are also shown in Table 7.

Table 7. Calculated Mulliken, electrostatic and natural atomic charges and the electrostatic potential surfaces for CxTP and PhTP molecules

Heteroatom	Charges (e)			Electrostatic potential surfaces*
	Electrostatic	**Mulliken**	**Natural**	
CxTP				
N1 Phenothiazine	-0.406	-0.594	-0.426	
S1 Phenothiazine	-0.116	0.183	0.355	
N2 C=N	-0.285	-0.220	-0.262	
N3 -N-H	-0.129	-0.483	-0.440	
N4 thiazole	-0.560	-0.500	-0.491	
S2 thiazole	0.012	0.270	0.426	
O1 -OEt	-0.297	-0.457	-0.540	
O2 C=O	-0.528	-0.505	-0.607	
PhTP				
N1 Phenothiazine	-0.386	-0.594	-0.426	
S1 Phenothiazine	-0.118	0.181	0.354	
N2 C=N	-0.271	-0.217	-0.259	
N3 -N-H	-0.142	-0.482	-0.439	
N4 thiazole	-0.533	-0.529	-0.520	
S2 thiazole	-0.011	0.255	0.416	

*By convention, the red colour from the electrostatic potential surfaces represents the negative potentials, blue colour represents the positive potentials, while orange, yellow and green colours depict intermediate values of the potential.

The atomic charges values listed in Table 7 show that N and O atoms possess negative charges, whereas S atom bears preponderantly positive charges. According to the electrostatic potential values, the electron rich regions which are subject to the electrophiles attack in HCl solution are N4 (-203.0 kJ mol^{-1}), O2 (-176.2 kJ mol^{-1}), N2 (-126.3 kJ mol^{-1}) for CxTP and N2 (-137.8 kJ mol^{-1}) and N4 (-139.3 kJ mol^{-1}) for PhTP, respectively. Based on these results, the possible protonation reactions of the investigated phenothiazinyl-thiazolyl-hydrazine derivatives occurring in HCl are presented in Scheme 1.
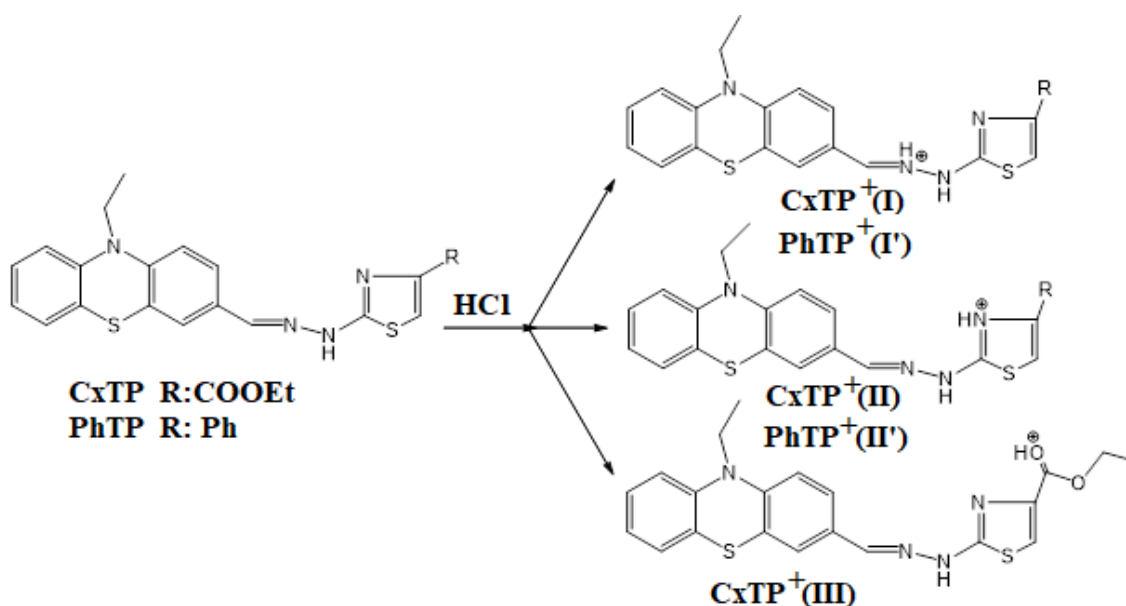
Scheme 1. The possible protonation reaction of the phenothiazinyl-thiazolyl-hydrazine derivatives in acidic solution

Since all protonated species of CxTP and PhTP would coexist in HCl solution and might interact with C-steel surface, it was interesting to investigate the influence of the protonation on their molecular structures and properties. The quantum chemical parameter calculated for the protonated forms of the phenothiazinyl-thiazolyl-hydrazine derivatives and their electron density distribution in HOMO and LUMO frontier molecular orbitals are presented in Table 8.

Comparing the total energy values, E calculated for all protonated forms of the two organic compounds, *i.e.* the cations **I, II, III** generated from CxTP and **I', II'** generated from PhTP (Scheme 1), it could be observed that the cationic species CxTP$^+$(**II**) and PhTP$^+$(**II'**) present the lowest E values (Table 8), which means that they are the most stable ones. The energy gap values between the protonated forms (E_{II}–E_I, E_{II}–E_{III} and $E_{II'}$–$E_{I'}$) also confirm their presence in acidic solution, probable with an excess of CxTP$^+$(**II**) compared to the other cationic forms of CxTP. The same observation could be made for PhTP, where the PhTP$^+$(**II'**) cation might prevail in the acidic solution over the PhTP$^+$(**I'**).

Table 8. Theoretical quantum chemical parameters of the protonated phenothiazinyl-thiazolyl-hydrazine derivatives and the typical HOMO and LUMO densities distribution

Molecule	E (kcal/mol)	E_{HOMO} (eV)	E_{LUMO} (ev)	ΔE (eV)	HOMO	LUMO
CxTP⁺(I)	-1241530.91	-8.34	-5.94	2.40		
CxTP⁺(II)	-1241534.75	-7.50	-5.04	2.46		
CxTP⁺(III)	-1241515.75	-6.99	-6.07	0.92		
PhTP⁺(I')	-1218858.54	-8.06	-5.87	2.19		
PhTP⁺(II')	-1218861.71	-7.40	-4.80	2.60		

The higher tendency of the nitrogen N4 from CxTP to be involved in the protonation correlated with the lower energy of the corresponding CxTP⁺(**II**) cation generated in this process confirmed the experimental results, which showed that CxTP exerts better inhibition properties compared to PhTP.

The E_{HOMO} and E_{LUMO} values of the protonated forms of CxTP and PhTP are lower compared to the corresponding values of the neutral inhibitors, which is also compatible with the experimental results. Moreover, the protonated molecules present smaller ΔE values compared to the neutral compounds, confirming that the inhibiting behaviour of the phenothiazinyl-thiazolyl-hydrazine derivatives in HCl is due to the adsorption of their protonated forms on C-steel surface.

Although all protonated forms of the phenothiazinyl-thiazolyl-hydrazine derivatives from Scheme 1 might interact with the C-steel surface during the inhibition process, for simplicity reasons, we will further limit our discussion to the most stable cations. As for example, the expected interactions between CxTP⁺(**II**) protonated molecule and C-steel surface are illustrated in Fig. 11.
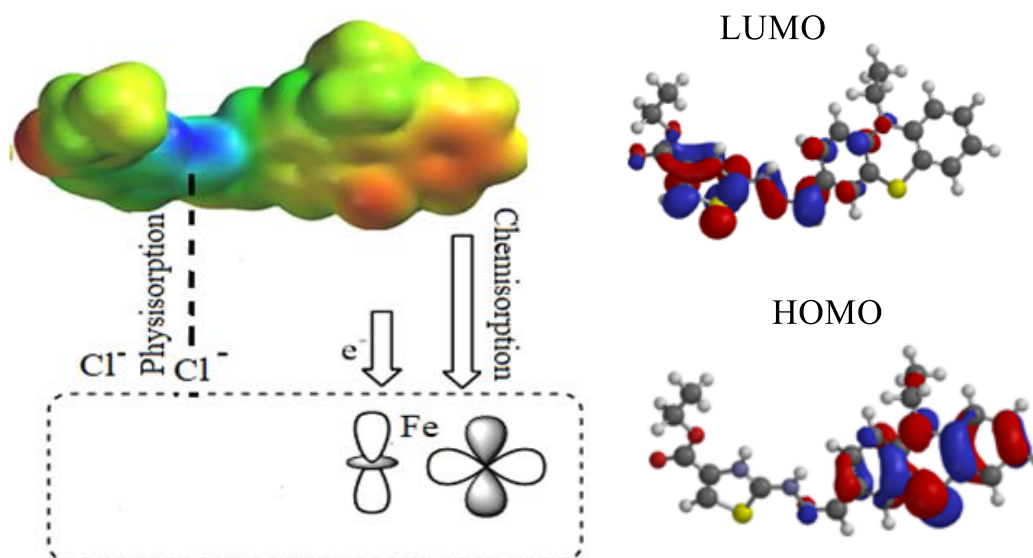
Figure 11. The possible interactions between **CxTP$^+$(II)** protonated inhibitor and iron surface

As shown in Fig. 11, the electrostatic potential surface (blue region) and the LUMO orbital indicate that the thiazole moiety from CxTP$^+$(**II**) bears positive charges and is mainly responsible for the electrostatic interactions. In the same time, the S atom and the aromatic rings from the phenothiazine core can be involved in electron transfer to the vacant *d* orbitals of Fe atoms, as suggested by the electrostatic potential surfaces (red region) and HOMO orbital of CxTP$^+$(**II**). Similar interactions could be assumed for PhTP$^+$(**II'**) protonated molecule and C-steel surface in 1.0 M hydrochloric solution.

3.6. Mechanism of corrosion inhibition

Generally, the corrosion inhibition mechanism in acidic solution is based on the adsorption of the inhibitor molecules on the metallic surface. Several factors affect the adsorption process, including the chemical structures of the inhibitors, the nature and charged surface of the metal, the aggressive electrolyte type, and the distribution of the charge over the whole inhibitor molecule [13].

As proved by DFT calculations, the investigated phenothiazinyl-thiazolyl-hydrazine derivatives exist in different protonated forms in HCl solution, which present several centres of adsorption on C-steel surface. Due to the complex nature of the interactions between the protonated inhibitors and Fe, it is impossible to advise a single adsorption mode of the phenothiazinyl-thiazolyl-hydrazine derivatives on C-steel surface [13]. Based on the obtained results, the following mechanisms were proposed to explain the corrosion inhibiting mechanism of studied organic inhibitors on C-steel in 1.0 M HCl solution.

The surface charge of the metal can be determined from the value of $E_{corr} - E_{q=0}$ (zero charge potential). In the case of Fe, the reported value of $E_{q=0}$ values is -530 mV *vs.* SCE in 1.0 M HCl [45]. In our study, the obtained value of E_{corr} is -475.1 mV *vs.* SCE. Hence, the C-steel surface bears positive charge in 1.0 M HCl, since the calculated value of $E_{corr} - E_{q=0}$ is +54.9 mV *vs.* SCE.

As the organic compounds exist in protonated forms in HCl, it is difficult to approach the positively charged C-steel surface due to the electrostatic repulsion [13]. Thus, it was assumed that the Cl⁻ anions could be first physically adsorbed on C-steel surface bringing an excess of negative charge near the interface [13, 42], which further favour the adsorption of the protonated molecules through electrostatic interactions on the cathodic sites of C-steel (Fig. 11). In other words, there may be a synergism between Cl⁻ and protonated inhibitors [46]. The physisorption of the protonated inhibitors on the negatively charged C-steel surface may compete with hydrogen ions reducing the rate of the cathodic reaction, without changing the hydrogen evolution mechanism.

In addition to physical adsorption, the protonated inhibitors may be adsorbed on C-steel via the chemisorption mechanism [47] involving the displacement of the water molecules from the metallic surface and donor-acceptor interactions of the free electron pairs of S atom and/or of the π-electrons of aromatic rings from the phenothiazine core and the vacant *d*-orbital of surface Fe atoms (Fig. 11). The unprotonated N atoms from the thiazole moiety and hidrazinyl bridge may also be involved in donor-acceptor interactions with the vacant *d*-orbital of Fe atoms. Finally, an adsorbed inhibitor film is formed on C-steel surface, acting as a barrier between the metal and corrosive solution and thus, reducing the dissolution rate.

These assumptions agree with the experimental results which revealed that the phenothiazinyl-thiazolyl-hydrazine derivatives are mixed-type inhibitors, acting by adsorption on C-steel surface involving two types of interaction, *i.e.* physisorption and chemisorption.

4. CONCLUSIONS

The following main conclusions can be drawn from the present study:

1. Phenothiazinyl-thiazolyl-hydrazine derivatives acts as efficient inhibitors for C-steel corrosion in 1.0 M HCl; their inhibition efficiencies increase with the inhibitors concentration, but slightly decrease at elevated temperatures and after 24 h of exposure to aggressive solution.

2. Potentiodynamic polarization indicates that the phenothiazinyl-thiazolyl-hydrazine derivatives behave as mixed-type inhibitors, with a predominant cathodic effectiveness. The maximum inhibition efficiencies of 91.6% for CxTP and 87.7% for PhTP were obtained at 150 µM concentration.

3. In EIS spectra, the inhibiting effect of the phenothiazinyl-thiazolyl-hydrazine derivatives results in an important increase of the impedance in the whole frequency domain. In the presence of the organic compounds, the processes taking place at C-steel interface are well described by a model containing two-time constants – one connected to the charge transfer and double-layer capacitance and the other to the inhibitor adsorption process.

4. The adsorption of organic molecules on C-steel surface obeys Langmuir adsorption isotherm. The calculated ΔG^0_{ads} values suggest that the adsorption process is spontaneous and involves both, physisorption and chemisorption modes.

5. SEM-EDX clearly verifies that the studied phenothiazinyl-thiazolyl-hydrazine derivatives significantly retard the C-steel dissolution process.

6. DFT calculations support the idea that the protonated forms of the phenothiazinyl-thiazolyl-hydrazine derivatives are involved in the inhibition mechanism.

References

1. M. Bouanis, M. Tourabi, A. Nyassi, A. Zarrouk, C. Jama and F. Bentiss, *Appl. Surf. Sci.,* 389 (2016) 952.
2. M. Outirite, M. Lagrenee, M. Lebrini, M. Traisnel, C. Jamab, H. Vezin and F. Bentiss, *Electrochim. Acta,* 55 (2010) 1670.
3. W. Zhang, R. Ma, H. Liu, Y. Liu, S. Li and L. Niu, *J. Mol. Liq.,* 222 (2016) 671.
4. R. Kumar, R. Chopra and G. Singh, *J. Mol. Liq.,* 241 (2017) 9.
5. D. Daoud, T. Douadi, H. Hamani, S. Chafaa and M. Al-Noaimi, *Corros. Sci.,* 94 (2015) 21.
6. Q. Qu, Z. Hao, L. Li, W. Bai, Y. Liu and Z. Ding, *Corros. Sci.,* 51 (2009) 569.
7. H. Hamani, T. Douadi, D. Daouda, M. Al-Noaimi, R.A. Rikkouh and S. Chafa, *J. Electroanal. Chem.,* 801 (2017) 425.
8. S.K. Shukla and M.A. Quraishi, *Corros. Sci.,* 52 (2010) 314.
9. W. Chen, H.Q. Luo and N.B. Li, *Corros. Sci.,* 53 (2011) 3356.
10. N.A. Wazzan, I.B. Obot and S. Kaya, *J. Mol. Liq.,* 221 (2016) 579.
11. Y. Tang, X. Yang, W. Yang, Y. Chen and R. Wan, *Corros. Sci.,* 52 (2010) 242.
12. N.A. Negm, Y.M. Elkholy, M.K. Zahran and S.M. Tawfik, *Corros. Sci.,* 52 (2010) 3523.
13. N.A. Negm, E.A. Badr, I.A. Aiad, M.F. Zaki and M.M. Said, *Corros. Sci.,* 65 (2012) 77.
14. M. Prajila and A. Joseph, *J. Mol. Liq.,* 241, (2017) 1.
15. R. Solmaz, *Corros. Sci.,* 52 (2010) 3321.
16. L. Boucherit, T. Douadi, N. Chafai, M. Al-Noaimi and S. Chafaa, *Int. J. Electrochem. Sci.,* 13 (2018) 3997.
17. P. Dohare, K.R. Ansari, M.A. Quraishi and I.B. Obot, *J. Ind. Eng. Chem.,* 52 (2017) 197.
18. N. Esmaeili, J. Neshati and I. Yavari, *J. Ind. Eng. Chem.,* 22 (2015) 159.
19. S. Hejazi, Sh. Mohajernia, M.H. Moayed, A. Davoodi, M. Rahimizadeh, M. Momeni, A. Eslami, A. Shiri and A. Kosari, *J. Ind. Eng. Chem.,* 25 (2015) 112.
20. M.M. Kabanda, L.C. Murulana and E.E. Ebenso, *Int. J. Electrochem. Sci.,* 7 (2012) 7179.
21. D. Özkır, K. Kayakırılmaz, E. Bayol, A. Ali Gürten and F. Kandemirli, *Corr. Sci.,* 56 (2012) 143.
22. H. Ashassi-Sorkhabi, D. Seifzadeh and M.G. Hosseini, *Corros. Sci.,* 50 (2008) 3363.
23. A.S. Fouda and A.S. Ellithy, *Corros. Sci.,* 51 (2009) 868.
24. L. Larabi, Y. Harek, O. Benalia and S. Ghalem, *Prog. Org. Coat.,* 54 (2005) 256.
25. A. Ignat, T. Lovasz, M. Vasilescu, E. Fischer-Fodor, C.B. Tatomir, C. Cristea, L. Silaghi-Dumitrescu and V. Zaharia, *Arch. Pharm. Chem. Life Sci.,* 345 (2012) 574.
26. W.J. Hehre, A guide to molecular mechanics and quantum chemical calculations, Wavefunction, Inc: Irvine CA (2003) USA.
27. A. Popova, M. Christov and A. Vasilev, *Corros. Sci.,* 53 (2011) 1770.
28. M. Tourabi, K. Nohair, M. Traisnel, C. Jama and F. Bentiss, *Corros. Sci.,* 75 (2013) 123.
29. F. Bentiss, F. Gassama, D. Barbry, L. Gengembre, H. Vezin, M. Lagrenee and M. Traisnel, *Appl. Surf. Sci.,* 252 (2006) 2684.
30. X. Wang, H. Yang and F. Wang, *Corros. Sci.,* 52 (2010) 1268.

31. I.D. Raistrick, J.R. MacDonald and D.R. Franceschetti, The electrical analogs of physical and chemical processes, in: J.R. MacDonald (Ed.), Impedance Spectroscopy Emphasizing Solid Materials and Systems, John Wiley & Sons (1987) New York, USA.
32. J.B. Jorcin, M.E. Orazem, N. Pébère and B. Tribollet, *Electrochim. Acta,* 51 (2006) 1473.
33. J. Aljourani, K. Raeissi and M.A. Golozar, *Corros. Sci.,* 51 (2009) 1836.
34. H.M. Abd El-Lateef, A.M. Abu-Dief, L.H. Abdel-Rahman, E.C. Sanudo and N. Aliaga-Alcalde, *J. Electroanal. Chem.,* 743 (2015) 120.
35. Z. Hu, Y. Meng, X. Ma, H. Zhu, J. Li, C. Li and D. Cao, *Corros. Sci.,* 112 (2016) 563.
36. X. Li, S. Deng, H. Fu and X. Xie, *Corros. Sci.,* 82 (2014) 4261.
37. F. Bentiss, M. Lebrini and M. Lagrenée, *Corros. Sci.,* 47 (2005) 2915.
38. X. Luo, X. Pan, S. Yuan, S. Du, C. Zhang and Y. Liu, *Corros. Sci.,* 125 (2017) 139.
39. F. Zhang, Y. Tang, Z. Cao, W. Jing, Z. Wu and Y. Chen, *Corros. Sci.,* 61 (2012) 1.
40. A. Popova, M. Christov and A. Vasilev, *Corros. Sci.,* 94 (2015) 70.
41. M. El Azzouzi, A. Aouniti, S. Tighadouin, H. Elmsellem, S. Radi, B. Hammouti, A. El Assyry, F. Bentiss and A. Zarrouk, *J. Mol. Liq.,* 221 (2016) 633.
42. F. Bentiss, M. Lebrini, M. Lagrenee, M. Traisnel, A. Elfarouk and H. Vezin, *Electrochim. Acta*, 52 (2007) 6865.
43. I.B. Obot, E.E. Ebenso and M.M. Kabanda, *J. Environ. Chem.,* 1 (2013) 431.
44. G. Banerjee and S.N. Malhotra, *Corrosion,* 48 (1992) 10.
45. X. Li, S. Deng and H. Fu, *Corros. Sci*., 53 (2011) 309.
46. A. Fitoz, H. Nazır, M. Özgür (nee Yakut), E. Emregül and K.C. Emregül, *Corros. Sci.,* 133 (2018) 451.